Finite element analysis of the thermal bending of a chilled cast thermo roll

THOMAS WIDMAIER, JUKKA PIRTTINIEMI, ESA PORKKA, PANU KIVILUOMA, AND PETRI KUOSMANEN

ABSTRACT: A previously-created roll model based on the ultrasound measurements of a chilled cast iron thermo roll of a soft calender was used to create a finite element (FE) model of the same roll. The FE analysis was used to simulate the behavior of the roll when heated and in changing operating conditions. The main interest was to study the thermal bending of the roll model. The simulated behavior was consistent with known behavior of the thermo rolls in general, and when compared to actual measurements carried out in the calender, the results of the simulation showed similar behavior between the roll model and the actual roll. The main difference was in the absolute value of the bending, but the bending directions were practically the same. These results are promising for future research to develop methods to avoid or minimize the negative effects of the thermal deformations in thermo rolls.

Application: This paper discusses some of the phenomena caused by temperature changes in paper machine thermo rolls. The studied phenomena include mainly thermal deformations, i.e., bending. This study is relevant to finding the cause for some calender-related problems, including thermo rolls.

The thermo rolls belong to the family of heated rolls in the paper industry. They are used to heat up the paper web passing through a calender. The heat improves the formability of the paper, thus improving the efficiency of the calendering. For many decades, chilled cast iron thermo rolls have been successfully used in calenders of paper machines. In 2004, the proportion of chilled cast iron thermo rolls amounted to 99% of all thermo rolls in the paper industry [1]. Even though the number of forged steel thermo rolls and other thermo roll types is slowly increasing, the number of the chilled cast thermo rolls is still dominant. Chilled cast iron has been used for roll shell material, mainly because of its good manufacturability and low material cost. Thermo rolls have an undesirable tendency to deflect when heated to the operating temperature. This temperature dependent deflection is also called thermal bending. Because of the inhomogeneous roll shell material, the chilled cast thermo rolls are more prone to this phenomenon than some other roll types.

The bodies of the chilled cast thermo rolls have a layered structure with three different layers (**Fig. 1** [2,3], left). On the surface, they have a white iron layer and on the inside, a grey iron layer. Between the two main layers, there is an intermediate zone (also called mottle iron layer), where the content of mainly white iron changes to mainly grey iron (Fig. 1, left). The layered structure with varying layer thicknesses is a byproduct of the casting process [4]. The average thickness of the white iron layer in paper machine rolls is typically 8 to

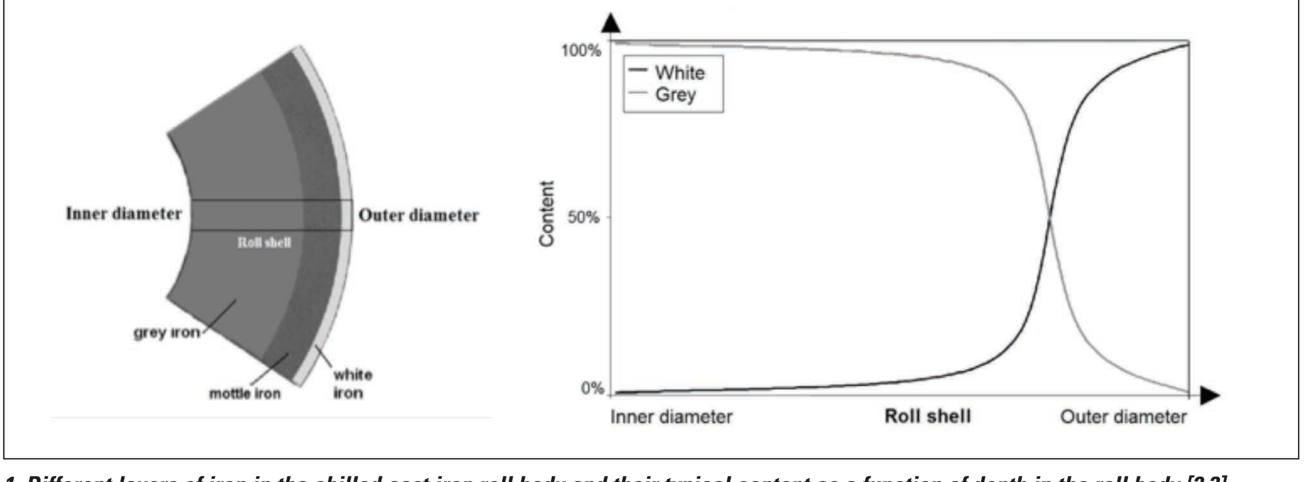

1. Different layers of iron in the chilled cast iron roll body and their typical content as a function of depth in the roll body [2,3].

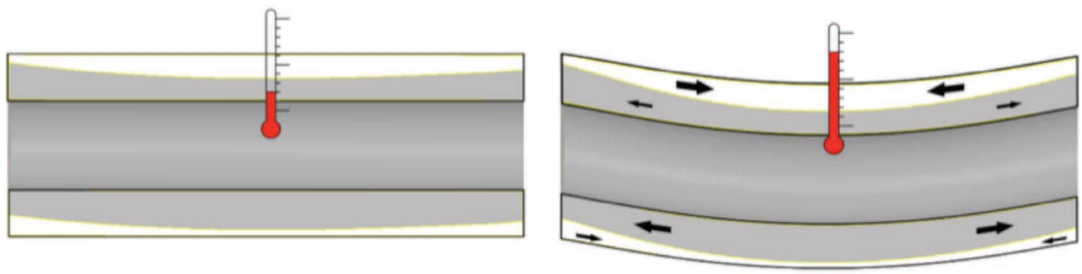

2. As temperature changes, thermal bending of the thermo roll is caused by the uneven layer thickness of white iron.

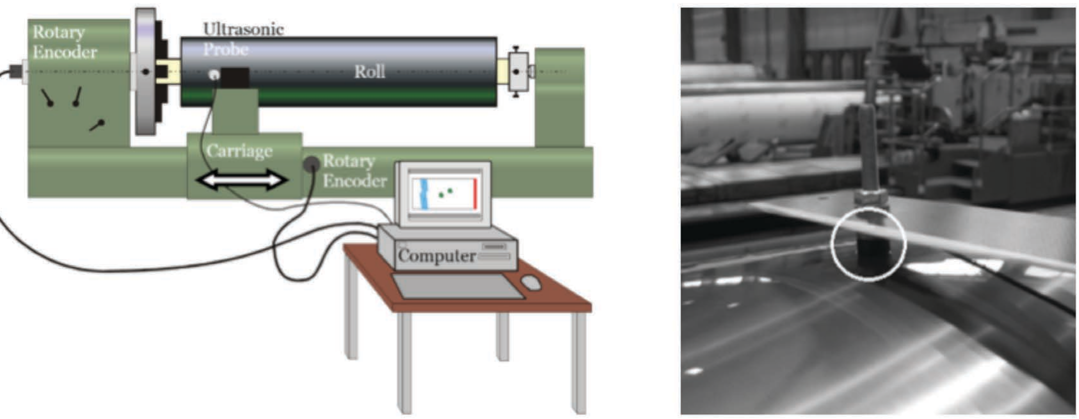

3. Principle of the ultrasonic measurement system (left) and the ultrasonic probe on the roll surface (right, circled). The rotary encoders give the coordinates of the ultrasound probe during measurement.

24 mm [5,6]. The mottle iron layer is thicker, but there are no clear boundaries between the layers, as it can be seen in Fig. 1 (right). The rest of the body is grey iron.

Thermal bending is caused by the uneven layer thickness of white iron. The thermal expansion coefficient of white iron is smaller than that of grey iron. If the roll is heated, it will deflect because of the forces that caused the uneven thermal expansion of the layers (**Fig. 2**). The direction and form of the deflection is determined by the layer distribution and temperature distribution in the roll body. Normally, there is no deflection in the rolls at room temperature.

There are several types of thermo rolls, and the most common types are center bore rolls, displacer type rolls, and peripherally drilled rolls. The working principle of these thermo rolls is based on hot heating fluid flowing through the roll body, i.e., the roll is heated from inside. Modern thermo rolls are mainly peripherally drilled rolls or displacer type rolls [7,8].

Peripherally drilled rolls have usually 15 to 50 bores that are 20 to 60 mm from the roll surface. The diameters of these bores are 25 to 50 mm [7]. The length of the bores is the same as the length of roll body, i.e., up to 12 m. There are many designs for the heating fluid passages, ranging from one bore per pass to three or more connected bores. The name of the design gives the number of the connected passages: mono-pass, duo-pass, tri-pass, etc. The heating fluids used with the thermo rolls are water, steam, or thermal oil. Some passage arrangements are presented in the book edited by Jokio [6], in the articles by Zaoralek [9,10] and Grosskreutz [11], and in the patent from von Schweinichen [12]. The heat transfer from the heating fluid to the roll can be made more effective if the turbulence of the fluid is increased. This can be done by special inserts in the passages. The inserts are called turbulators [8,12].

This study discusses the use of a previously-created roll model [4] in simulating the thermomechanical behavior of a chilled cast iron thermo roll. Ultrasonic measurements were used to acquire dimensions of the peripherally drilled bores in the shell of the roll body. Ultrasound was also used in measuring the layer thickness of the white iron layer on the roll surface. The ultrasonic measurement principle is shown in **Fig. 3**. This study is about the peripherally drilled chilled cast iron thermo rolls, but some of the results can be extended to other roll types, too.

METHODS

A chilled cast iron thermo roll (**Table I**) was used as a test roll and as a basis for the roll model. The test roll was the upper roll of a soft calender. The heating passage design was

Total length	9810 mm
Body length	7690 mm
Maximum paper web width	6660 mm
Nominal diameter	1067 mm
Shell thickness of the roll body	198 mm
Bearing length	8400 mm
Peripheral bore diameter	32 mm
Layer thickness of white iron	9 mm
Layer thickness of mottle iron	42 mm
Heating fluid	thermal oil
Design temperature for oil	249°C
Heating capacity	695 kW
Balancing speed range	0 to 388 min^{-1}

I. Dimensions and properties of the test roll.

duo-pass, and the roll had 40 peripheral bores. The roll was measured during normal operation and during maintenance. The ultrasonic measurements were carried out at a roll shop on a roll grinder. The run-out measurements were carried out in the soft calender. The run-out measurement method is discussed in the dissertation of Kiviluoma [13], and it is based on a sliding pad with an accelerometer, as in **Fig. 4**. The run-out values were obtained by double integration of the acceleration signal.

The calculation of the distribution of the white iron layer in the roll body is explained in the article of Widmaier et al. [4]. It is based on the reverse ultrasonic measurement of the wall thickness of the roll body. To simplify the calculations, the layer structure is reduced to two layers, assuming that one half of the mottle iron layer behaves like grey iron and the other half like white iron. If not otherwise mentioned, in the rest of this study the white iron layer is defined this way. The thickness variation of the white iron layer was from 27.0 mm to 33.3 mm. The average layer thickness was 30.3 mm (**Fig. 5**).

The depths of the peripheral bores in the roll were mea-

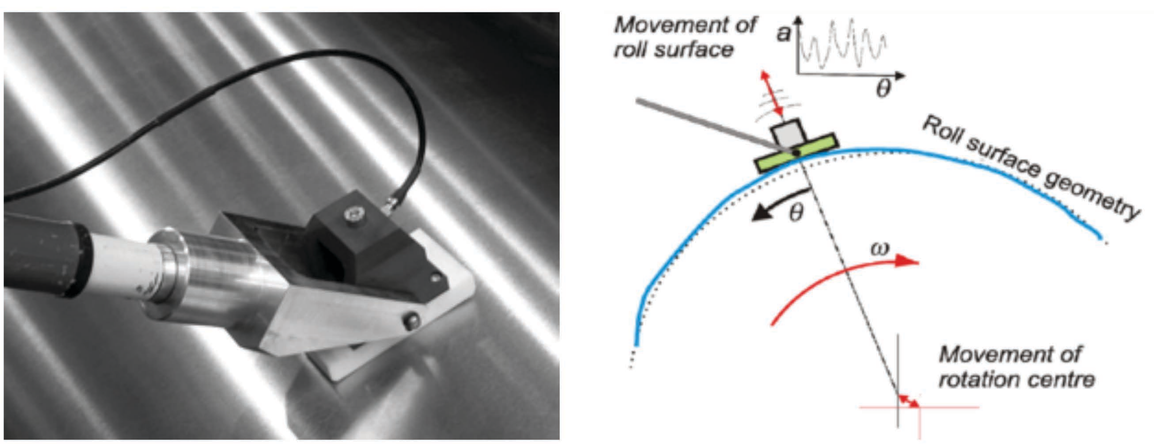

4. Left: in-situ run-out measuring device with accelerometer. Right: the measurement principle.

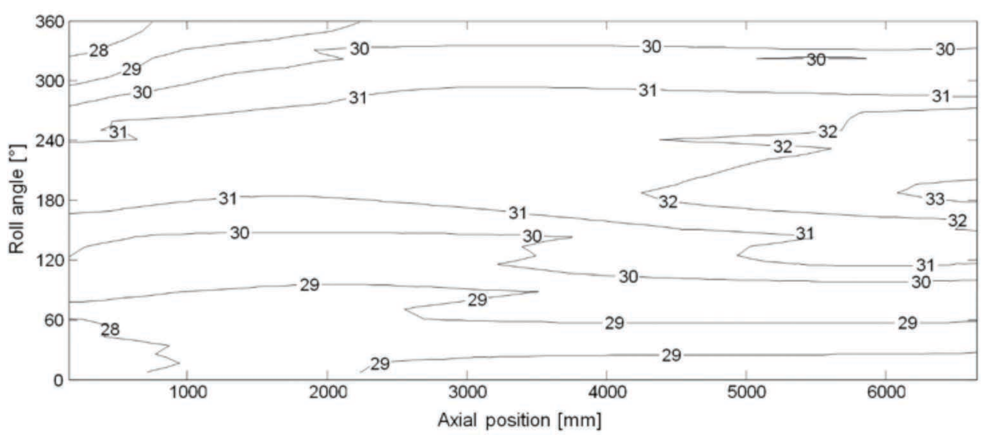

5. Map of the layer thickness variation (mm) of the white iron in the roll body of the test roll [4].

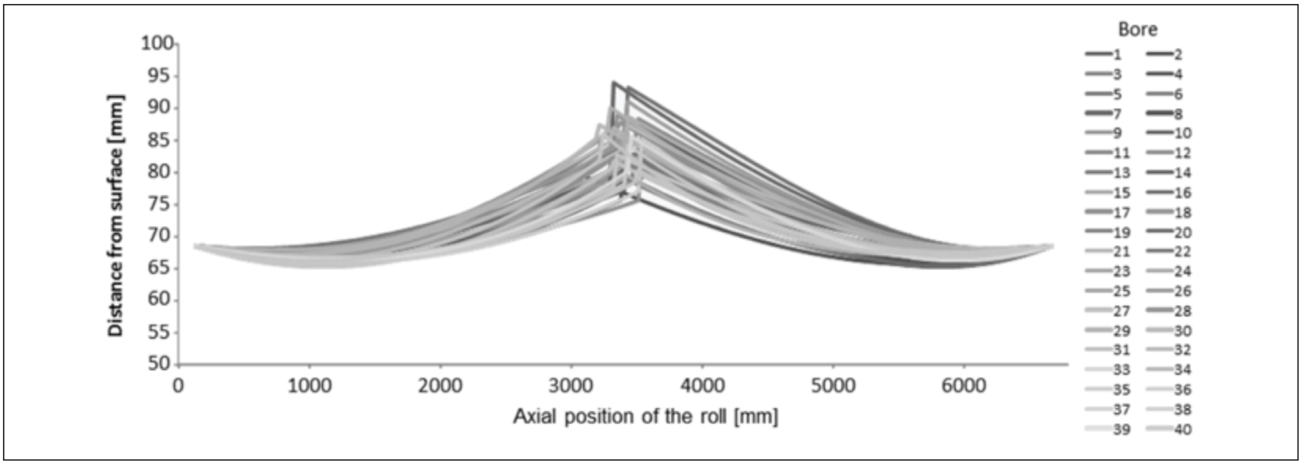

6. Bore depths of all the peripheral bores in the roll body [4].

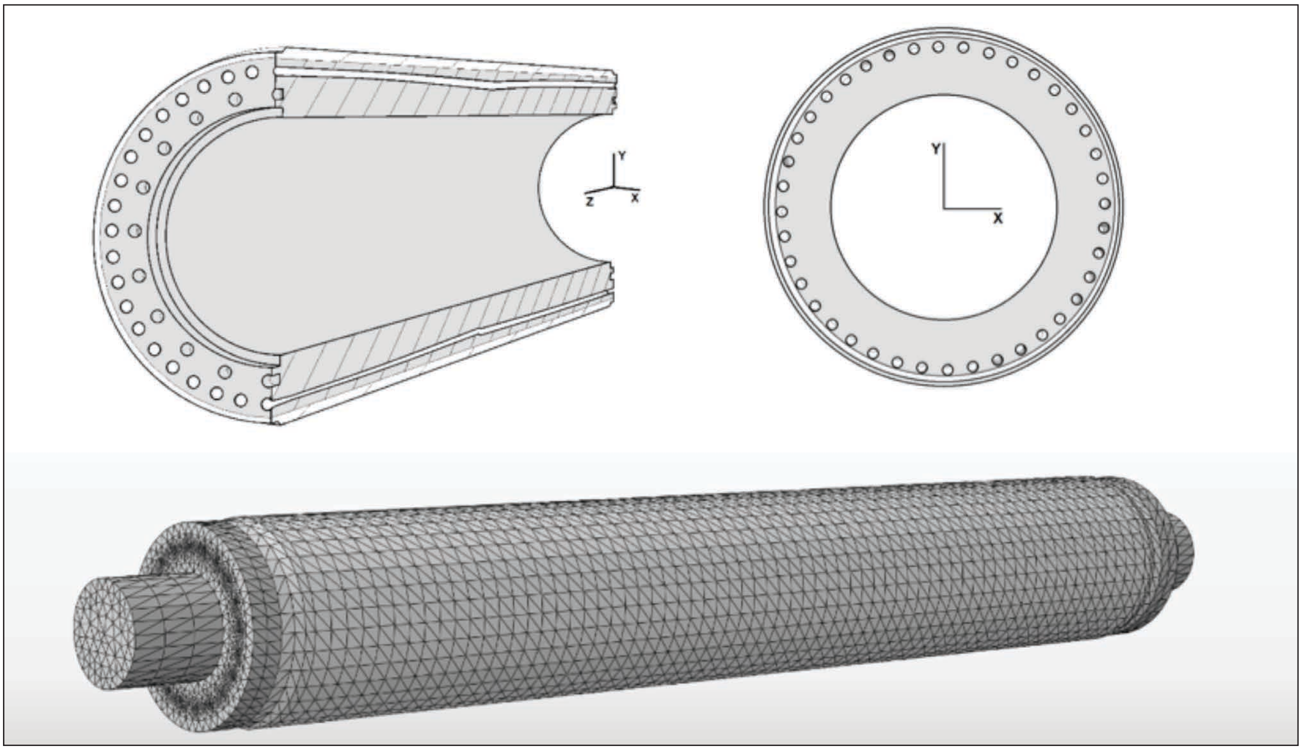

7. Top: 3D model of the thermo roll body in cut-in-half state and shown from the end. Bottom: the finite element (FE) model of the roll with the modelled journal parts attached. The used element type is a 4 node tetrahedron.

sured with ultrasound. The measured values show some meeting difficulties in the bores and some scattering in the bore depths (**Fig. 6**) similar to the results found in the literature [14]. The measurement of the depths of the bore centerlines with ultrasound is described by Widmaier et al. [4].

Finite element model of the roll

The dimensions for roll model were taken from the test roll. The white and grey iron layer models were created with the help of the ultrasonic layer border (Fig. 5). The layer border surface was the outer surface of the grey part and the inner surface of the white part. The solid model with 40 protrusions of the peripheral bores was used to cut the fluid channels into the grey iron part. Each measured peripheral bore centerline was used as a trajectory of a protrusion for the bore model. The protruded section was a circle with the diameter of 32 mm. Two different roll journals of steel were added. The journals were also equipped with heating fluid passages. One of the journals was the service side journal and the other was the drive side journal. The journals were fastened with 20 simplified M32 x 200 bolts each. The part to simulate the heating oil in the model was created from the cut-out model for the bores.

The 3D model (**Fig. 7**, bottom) was exported to Abaqus

Material	E, GPa	ν	ρ, kgm^{-3}	k, $Wm^{-1}K^{-1}$	c_p, $Jkg^{-1}K^{-1}$
White iron	180	0.27	7694	20.76	586.6
Mottle iron	140	0.27	7583	31.15	544.6
Grey iron	120	0.27	7334	45.68	502.8
Steel	207	0.30	7835	48.17	628.5

II. Material values of the iron phases [2,8,15,16].

Temperature, °C	h, $Wm^{-2}K^{-1}$
40	405
100	980
150	1452
170	1632
200	1900
250	2300

III. Temperature-dependent oil-shell gap conductance (h) interaction [17].

Interaction	Interaction type	h, $Wm^{-2}K^{-1}$
Oil-insulated bores	Gap conductance	40
Body – journal	Gap conductance	5000
Paper web area	Surface film condition	73
Cylinder faces of journals	Surface film condition	72
Other surfaces of journals	Surface film condition	25

IV. Temperature-independent heat transfer coefficients of the interactions.

Unified FEA software (Dassault Systemes; Vélizy-Villacoublay, France) for the finite element (FE)-based thermomechanical analyses. The individual parts (shell, journals, bolts and oil) were meshed. The used element type was a solid 4 node linear tetrahedron. After the meshin,g the total number of the nodes was 77170, and the total number of the elements was 333174 in the FE model. The used element type is suitable for the calculation of the node displacements in the model, even though it is one of the simplest 3D element types, and thus can give distorted geometry changes in small scale. The reduced number of nodes reduces the calculation time of the analysis.

The used material values are in **Table II**. The mass of the model (Fig. 7, bottom) was 30385 kg, which is close to the given mass of the actual roll (30500 kg). In the FE analyses, the roll heating was simulated by changing the temperature of the nodes in the oil part to the desired operating temperature. The starting temperature was always the room temperature (20°C). This was done in heat transfer steps. After the analysis was run, the resulting database contained the temperatures of the nodes as a function of time. In the heat transfer steps, the elements in the model were of DC3D4 element type (4 node tetrahedron) of Abaqus software. During the heat transfer analysis, the parts of the model had several interactions. **Table III** lists the values of heat transfer from the oil to the roll body, which are defined as temperature dependent. Table IV lists the rest of the interactions, which are defined as temperature independent.

The gap conductance for the thermal oil-to-roll body interaction was calculated as the film coefficient in a pipe with turbulent oil flow. The used oil flow speed was 1.9 m/s. This calculation is explained in the article of Zwart and Farrell [16]. The use of a turbulator increases the heat transfer coefficient value. Based on the information provided by the thermo roll manufacturer, it was concluded that the used turbulators increase the heat transfer coefficient by a factor of two. The roll had also insulation around the bores at the roll shell ends. The heat transfer coefficient for this part of the oil-to-shell contact was taken also from Zwart and Farrel [16], but increased slightly from 34.4 to 40 W/m^2K to reduce the large temperature drop on the roll surface in the end area of the roll body.

Nominal Oil Temperature, °C	Input Temperature, °C	Output Temperature, °C
100	100	98
150	150	147
170	170	165
200	200	197
249	249	240
250	250	246

V. Input and output temperature of the oil.

The drop in the temperature distribution of the oil part was linearly distance dependent, i.e., the temperature dropped linearly from input to output. This simulated the cooling of the oil. **Table V** lists the input and output temperatures of the oil at the set oil temperatures. The temperature difference between input and output temperature for the 100°C, 150°C, 200°C, and 250°C oil temperatures is smaller than for the 170°C and for 249°C oil temperatures, because

Set Oil Temperature, °C	Heat Surface Flux, kWm^{-2}	Equivalent Heat Load per Roll Length, kWm^{-1}
170	9.0	30.1
190	10.5	35.2
249	15.5	51.9

VI. Heat surface fluxes and the corresponding heat loads used in the analyses.

the latter cases simulate paper production conditions where the temperature drop in the oil is larger.

The calculation of the film coefficient for the heat transfer into the air from the rotating roll surface is also explained in the same article of Zwart and Farrell [16]. For the calculations of the film coefficients, a rotation speed of 5.8 Hz of the roll was used. The calculation of the thermal contact conductance between the roll body and the journals is explained by Yovanovich [18]. Too many of the needed parameters for the calculation were missing (turning pitch, tool radius, etc.), so an estimate of the coefficient was made based on values found in several research papers.

The heat load during paper production was simulated by a surface heat flux from the paper web area of the roll. The magnitude of the heat flux was chosen so that the final surface temperature was close to measured temperatures and close to temperatures provided by the roll manufacturer. The heat flux values are listed in **Table VI**. The equivalent heat load in the same table tells how much of the heat was taken by the paper web per roll length. The total heat transferred through the roll is more than in Table VI, because the heat also escapes through the other parts of the roll. The standard heat transfer simulation analysis had 7 steps, with a total duration of 10 h of simulated operation. The steps were named: *StartTemperature, HeatOn, Heating, PaperWebOn, PaperProduction, NipOpen*, and *NoProduction*. The other analyses simulated the effect of the decreasing heat load of the paper web and the effect of the changing oil temperature. **Table VII** lists the names and main parameters of the individual steps.

After the temperature field in the roll was calculated in the heat transfer analyses, a displacement database was calculated for the same model, but without the oil and the bolt parts. The temperature field for this analysis was taken from the heat transfer analysis results database. The element type was changed to C3D4, which is a 3D stress element, and it can be used for displacement calculations. The node locations and the mesh did not change due to this.

The journal ends were tied to the roll body ends in a small ring around the bolt holes. The width of the ring was 40 mm. Otherwise, the journal-to-body contact was defined as a hard contact. The roll models were simply supported at the journal ends. This means that the center point of the axis end of the service side journal is locked in all directions and the axis end of the other journal is locked in radial directions (XY plane). A supplementary node in the service side journal axis end was locked in the radial direction (XY plane). These boundary conditions allowed the roll to axially expand and kept it from rotating, but did not prevent the bending of the roll.

The coefficients of thermal expansion used for the white and grey iron are shown in **Table VIII**. As the table shows, both iron layers had temperature-dependent thermal expansion coefficients, and in addition, the white iron layer had an orthotropic (direction-dependent) thermal expansion coefficient during the analyses.

Step Name	Duration	Heat	Heat load	Purpose/simulates what?
StartTemperature	60 s	no	no	Whole model set to 20°C
Heating	3 h			This period has 2 steps
HeatOn	10 min	yes	no	Oil heat is turned on
Heating	2:50 h	yes	no	Roll is heated
Paper production	6 h			This period has 2 steps
PaperWebOn	10 min	yes	yes	Paper production starts
PaperProduction	5:50 h	yes	yes	Paper production
Decreasing load	3 h	yes	yes	Heat load decreases slowly
Changing temperature	3 h	yes	yes	Temperature fluctuates
Nip open	1 h			This period has 2 steps
NipOpen	10 min	yes	no	Nip opens
NoProduction	0:50 h	yes	no	Conditions after production

VII. Durations of the analysis steps and heat conditions.

Temperature, °C	Grey iron, °C-1	White Iron, °C-1	
		Radial Direction (XY)	Axial Direction (Z)
50	10.0E-6	9.0E-6	7.5E-6
100	11.0E-6	9.3E-6	6.9E-6
150	11.0E-6	9.3E-6	6.2E-6
200	11.0E-6	9.3E-6	5.5E-6
250	11.0E-6	10.0E-6	6.6E-6
300	11.8E-6	10.8E-6	7.8-6

VIII. Temperature-dependent thermal expansion coefficients for the used iron layers. Grey iron thermal expansion coefficient is isotropic and white iron thermal expansion coefficient is orthotropic [2].

Fourier analysis

One of the most common Fourier analyses is done with the fast Fourier transform (FFT) algorithm originally developed by Cooley & Tukey [19]. The inverse FFT algorithm can be used to compose the original measurement signal in the time domain from these complex numbers. Filtering of some unwanted frequencies or components is straightforward. The complex number representing the unwanted frequency or component is set to zero before the inverse FFT, an example of which is shown by Mosier-Boss et al. [20]. In the analyzed measurement signals of our research, the FFT algorithm is used for both identifying certain harmonic components and for filtering purposes.

Analysis software

The FE analyses were solved with the Abaqus FEA software. The analysis procedure used was the Abaqus/Standard. For all the analysis steps, the step type was “static, general”. The starting condition for each general analysis step is the ending condition from the last step, with the state of the model evolving throughout the history of the analysis steps. The FE analyses produced result files with all the results from each analysis. From these results, a report file was generated with the Abaqus CAE software. In the report file, all the node displacement and all the node temperature results were stored. One report file contained the results from all the simulation steps with their time increments from one analysis run. The presented results were calculated from the report file together with the analysis input file. The input file was used to locate the surface nodes in the nip area of the roll. During this work, over 200 individual FE analyses were run. The report file sizes ranged from ~400 megabytes to over 800 megabytes, depending on the extent of the analysis. A software program was developed to calculate the displacement of the surface nodes in the radial direction (XY plane) from nine cross sections of the roll body in all analysis time steps. At the same time, it calculated the average temperature of the all surface nodes in the nip area. The radial direction was chosen, because the axial direction (Z) was not relevant for the study of the thermal bending. Still, the thermal expansion in the axial direction was the most dominant expansion direction; e.g., at 200°C it was over 10 mm.

The same software performed an FFT analysis of the individual cross section profiles. From this FFT analysis, the overall thermal bending can be observed from the 1st FFT term of middle cross section if the ends of the roll shafts are fixed like in these simulations. The 1st term, also known as the 1st harmonic component, gives the amplitude and the direction of the bending.

RESULTS

The results from the model analyses and simulations are presented as graphs. Some results are compared to measurements. Simulation results are presented as a function of time and as a polar plot. The presented results are the amplitude and the phase of the 1st harmonic component of the displacement of the circumferential surface nodes in the middle cross section. The time-based graphs also show the average temperature of the all surface nodes at the roll shell in the nip contact area. The time scale is divided into periods like heating, paper production, and nip open. These periods are explained in Table VII. If not otherwise stated, only during the paper production period is a heat load taken from the roll nip surface. During the heating period, oil temperature changed to operating temperature with a speed of 2°C/min. This value was found in the literature for modern thermo rolls [10,21]. Also, graphs from nine cross sections are presented to show the bending profile in the nip surface of the whole roll length.

Time based simulations

Figures 8-9 show the results from the standard simulation set. The first figure always shows the amplitude, phase angle,

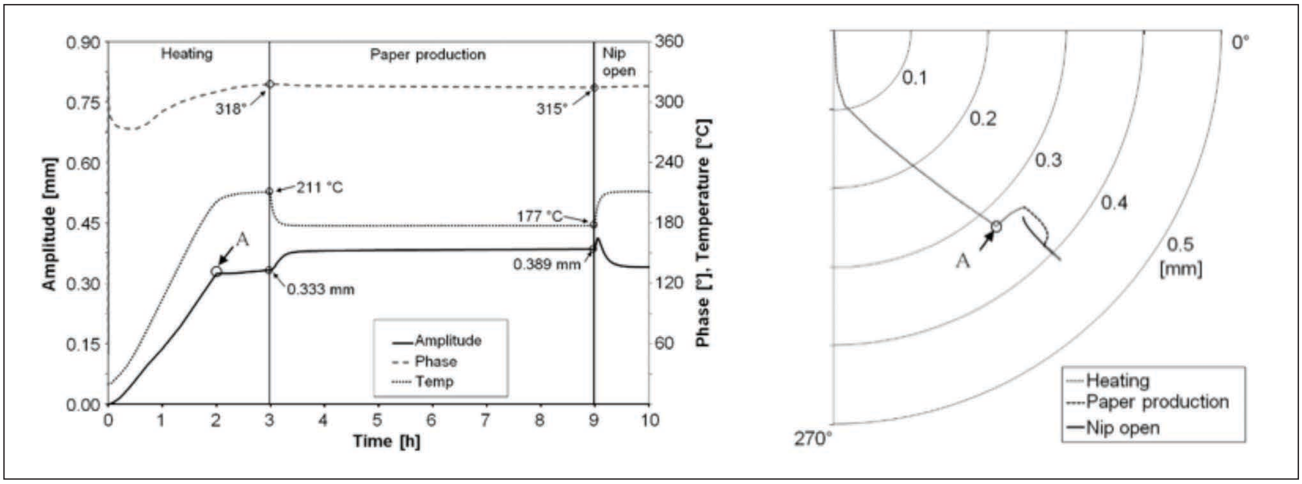

8. Left: thermal bending of the roll model and average surface temperature as a function of time, heating oil 249°C, and heat load 51.9 kW/m during production. Right: development of the left figure's thermal bending as a polar plot.

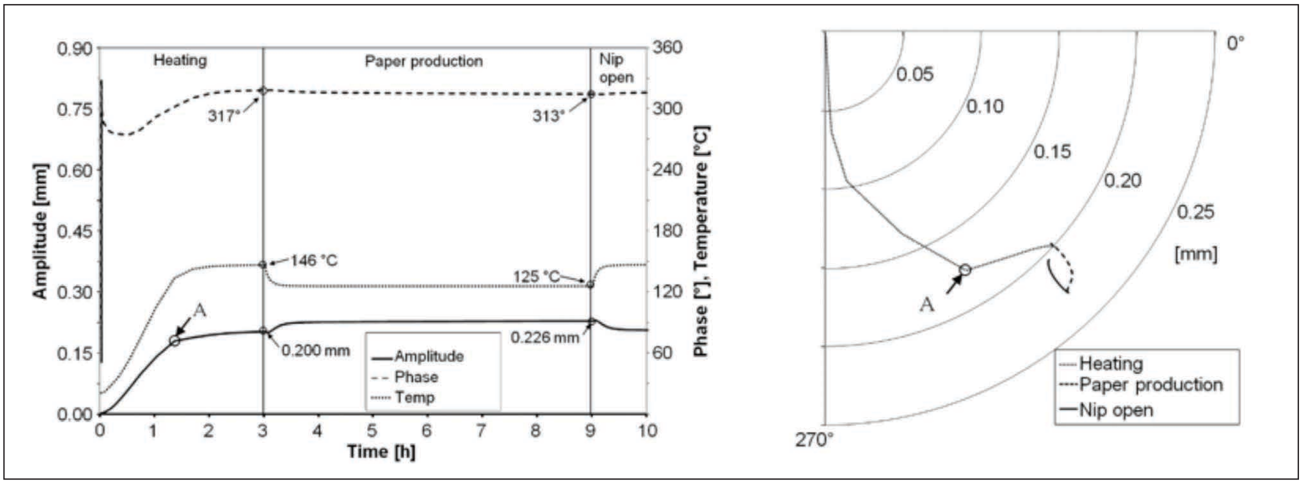

9. Left: thermal bending of the roll model and average surface temperature as a function of time, heating oil 170°C, and heat load 30.1 kW/m during production. Right: development of the left figure's thermal bending as a polar plot.

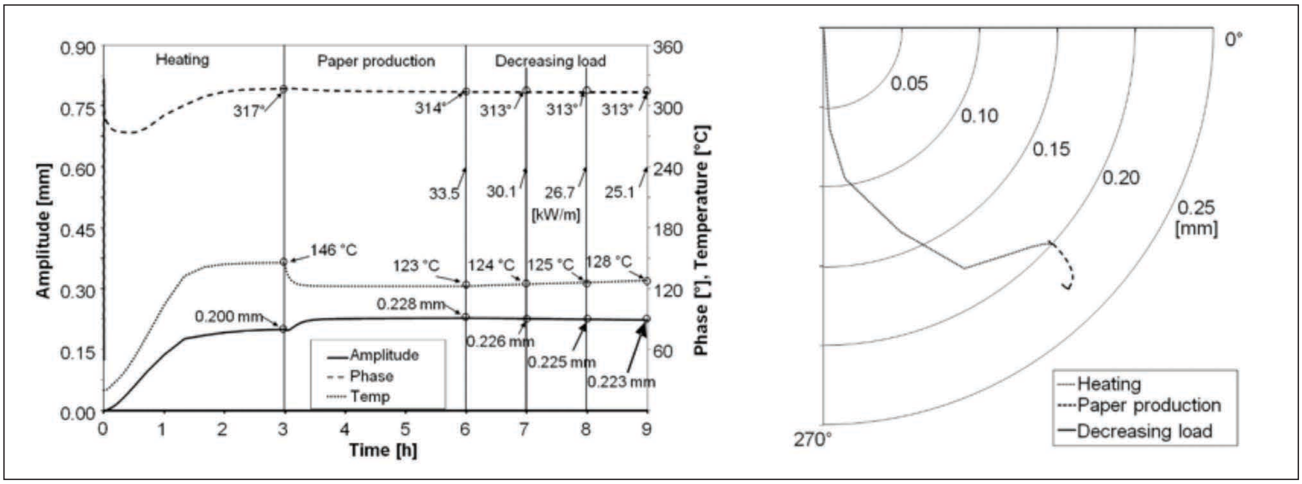

10. Left: effect of a slowly decreasing heat load (33.5 to 25.1 kW/m) with 170°C oil temperature. Right: development of the left figure's thermal bending as a polar plot.

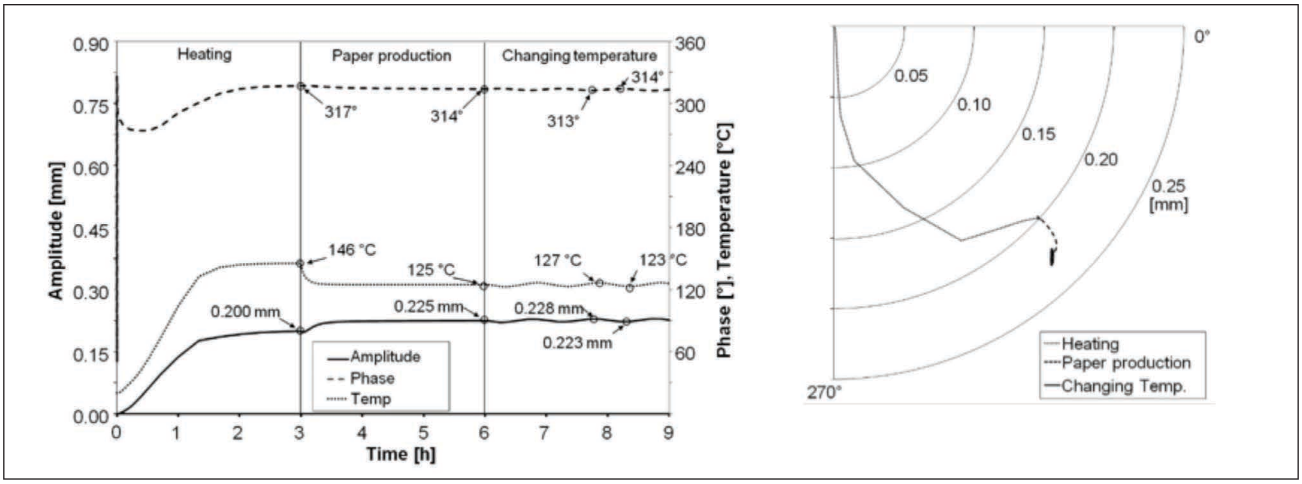

11. Left: effect of a slowly changing oil temperature (±4°C) with 170°C oil temperature. Right: development of previous figure's thermal bending as a polar plot.

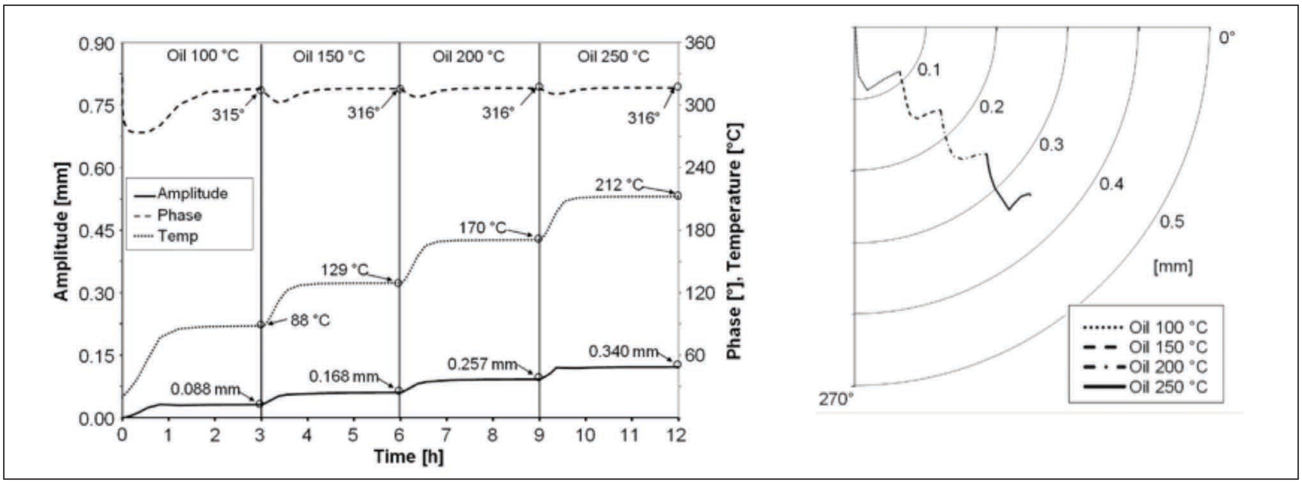

12. Left: heat up ramp, with four different oil temperature steps. Right: development of the left figure's thermal bending as a polar plot.

and temperature vs. time plot. This figure is then followed by a polar plot with the same bending data. The difference in the first two analyses was in the simulated oil temperature. The maximum temperature in the first analysis was 249°C. This temperature was chosen because it was the original design temperature of the roll (Fig. 8). In the second analysis, the maximum temperature was 170°C. This temperature was chosen because it is currently the temperature used in the paper mill (Fig. 9). The first two simulations present a simulation run with 3 h heat up time and 6 h production time. After the heat load is set to zero (simulates the nip open situation), the behavior was analyzed for 1 h. The polar plot shows the movement of the center point of the middle cross section during the simulation. A point A is shown in both graphs. This is provided to help visually synchronize both plots.

In **Fig. 10**, the nip open period was replaced by a slowly changing heat load period. The heat load changed from 33.5 to 25.1 kW/m in 3 h. The purpose of this simulation is to see effect of slight paper web variations like web speed, water content, bulk density, etc. **Figure 11** shows the effect of a slowly fluctuating oil temperature. This simulates the thermostat effect in the oil temperature control system of the roll. The temperature fluctuation was ±4°C. **Figure 12** presents a temperature ramp with four oil temperature steps. The roll model was heated with 100°C, 150°C, 200°C, and 250°C hot oil.

Comparison of simulated run-out and run-out measurements

The last set of results compares a range of simulated results with actual measurements. The first harmonic components of the node displacements from nine cross section profiles are presented in **Fig. 13**.

The simulation data is the same as in Fig. 12. The upper results are from the simulation, and they are taken from the end of the period with oil temperature of 250°C (after 12 simulated hours of heating). The lower graphs are from the

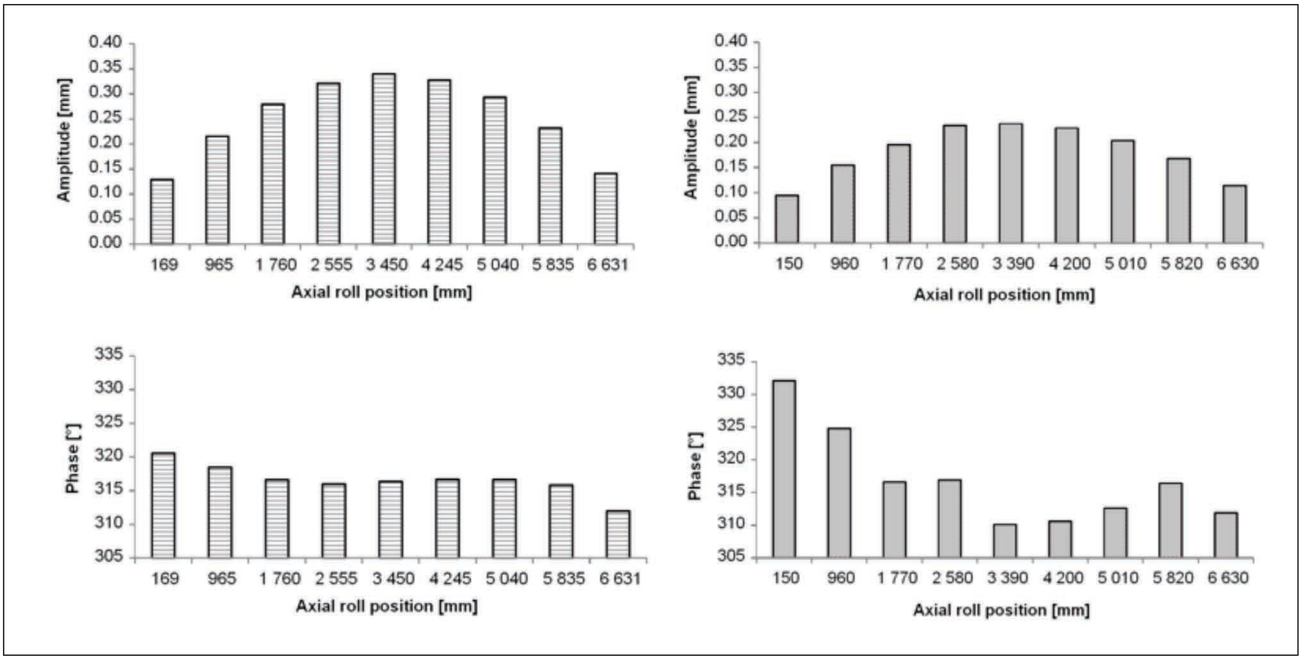

13. Amplitudes and phase angles of the 1st harmonic components from 9 cross sections. Left graph is from the simulation and right graph is from the run-out measurements.

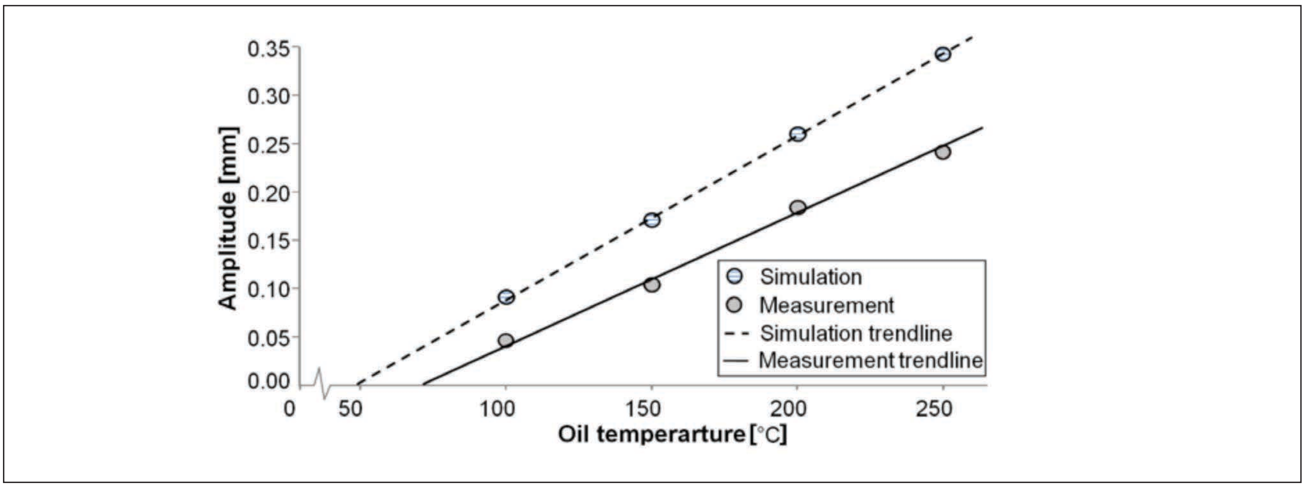

14. Comparison between a measurement and a simulation with the same oil temperatures.

run-out measurement in the calender. The oil temperature during the measurement was set to 250°C, and the rotating speed of the roll was 6 Hz.

Figure 14 shows the amplitude of the 1st harmonic component of the run-out measurement of the middle cross section profile of the roll [22]. The same figure shows the amplitude of the 1st harmonic component of the displacement in the surface nodes of the middle cross section of the roll model. The amplitudes are from the same heat ramp simulation as in Fig. 12. The speed of the oil heat up in the simulation was 2°C/min. The speed of the oil heat up during the measurements is not known. The roll was rotating during the measurements (6 Hz), and the simulated roll model was static, but the thermal effects were calculated as if the roll was rotating with 5.8 Hz. The thermal effects were mainly the surface film condition parameters for the cooling effect by the surrounding air during rotation.

The actual measurement was performed so that the temperature was set from the operator panel. The roll was considered to have reached the set temperature when the surface temperature of the roll was steady for 10 min. The temperature of the roll surface was measured with a handheld IR-thermometer from Fluke (Everett, WA, USA). Fig. 14 shows the development of the amplitude of the 1st harmonic component in the middle cross section of the roll in correlation with oil temperature.

DISCUSSION

The results from the simulations are consistent with previous studies and common knowledge about the behavior of the chilled cast iron thermo rolls. When compared to actual measurements, the distinct difference is in the amplitude. The phase angles (direction) of the bending are more similar, although the roll had a service visit between the run-out measurements and the ultrasound measurements for the roll model creation. During the service visit, the journals were removed, machined, and reattached, so there is no absolute guarantee that zero position for the roll angle was the same during the measurements, but normally the positions of the journals are fixed.

The change in the direction of the bending during the heating period probably comes from the bore depth variation. The bore depths vary in the roll body, thus delaying the temperature increase in some parts of the body. When the temperature differences have time to even out, the bending direction determined by the layer thickness variation then becomes the main direction. The delay in the settling time of the bending direction can also explain the greater variation in the phase angles of the actual measurement in Fig. 13. The results from the simulation are calculated from the same simulation step; i.e., the simulation time is the same for the data. In the actual measurement, there is a small delay between the measurements of the individual cross sections. The roundness profile of the actual roll can also affect the run-out measurement results. The average bending direction of the actual roll and the roll model are almost identical: actual is 316.9°, and the roll model is 316.6°.

The cooling of the surface during paper production increased the thermal bending of the roll model during simulation. This kind of behavior was observed before from measurements made from actual thermo rolls [23]. This behavior comes from the increased stress between the layers in the roll body.

The simulations with the decreasing heat load and the small variation in the temperature were performed to see the effect of these changes on the thermal bending. There have been some reports from paper mills that the direction of the bending has suddenly changed, e.g., by 180°. The performed simulations gave no explanation as to these reports. In the case of one of the reported bending direction changes, the roll journals had valves to affect the speed of the heating fluid flow. These valves can delay the heat up of the roll body in some parts of the roll, and so provide an explanation for the sudden change of the thermal bending direction. This was not simulated in the performed FE analyses. From the results of all the simulations, it can also be seen that a temperature change causes a change in the bending direction and in its amplitude, but a change in the heat load mainly causes a change in the bending amplitude. The change in the heat load affects the temperature in the roll more slowly than the heating oil. The heat transfer rate of the white iron layer is much less than that of the grey iron layer; i.e., the white iron layer acts as an insulator.

The reason for the difference in the amplitudes between the actual measurements and the simulated behavior could be in the chosen material values. The material properties are chosen from different sources found in the literature. The size of the thermal deflection of the roll is very sensitive to the values of the heat expansion coefficients. Also, the simplified structure has an effect on the behavior of the model. The values for the used material properties were for pure white iron and for pure grey iron. As it can be seen in Fig. 1, the thickness of the pure white iron layer is almost nonexistent. This means that at least the main material values for the white iron layer are too high (as for E) or too low (as for α). A better value for these can be obtained by the integration over the depth of the white iron content in the outer layer. Because of the larger thickness of the grey iron layer, the content of the white iron in the grey iron layer can probably be neglected; i.e., no change in the values for the grey iron is necessary. The used element type was one of the simplest. The 4 node tetrahedron element type is easy to use, but the results are not always reliable. The thermal bending of the roll model, and especially the amplitude, should be otherwise checked, either analytically or with another element type.

The nip pressure is also neglected in the model. The other roll in the calender will have an effect on the measured thermo roll. This effect is very likely dependent of the magnitude of the nip pressure, although other measurements made during this work showed almost no correlation between the nip load and the deflection in the allowed nip load range. The measurements presented in this study were all made in the nip open condition.

The thermal deflection causes an unbalance in the roll. If the roll rotates (as during the run-out measurements or as during paper production), this unbalance can increase the total run-out. The roll model experienced no centrifugal forces during the simulation, so this can explain some of the differences in the amplitudes.

During the simulation, the nodes of the oil part had the same temperature distribution in the end of the heat up period, paper production period, and the nip open period. In the actual roll, the temperature drop in the oil will be larger during the paper production period than in the other periods. This can have an effect on the thermal deformations in the roll model.

Also, the boundary conditions of the FE model can have a strong effect on the simulated thermal bending. The center nodes at the end of the shafts of the journals were fixed. The actual roll has a bearing around the shaft. Even though the distance between the fixed nodes in the simplified journals of the model and the distance between the bearings of the actual roll were the same, the forces or torque caused by the bearings are not the same as in the roll model. The effect of the chosen boundary conditions and possibly better alternatives should be studied further. The exact material properties in the roll should also be measured. Normally, this cannot be done from a production roll, because the dismantling of the roll is not allowed. Possible cooperation with the roll manufacturer can provide a solution to this problem.

CONCLUSIONS

The fact that the direction of the thermal bending of the roll and the roll model were almost identical gives the authors reason to believe that the roll modelling by ultrasound measurements can provide valuable information about the roll behavior, which would otherwise be very hard to obtain. The main difference between the simulated behavior of the roll model and the actual roll was in the magnitude of the bending. This was observable in the 1st harmonic component calculated from the cross-section profiles in the middle of the roll. The simulation was done by FE analysis. The service visit of the roll, where the journals were removed and reattached, is an unfortunate uncertainty factor in the results.

The presented case is from one roll only. The research should be expanded to cover several other rolls so that the correctness of the modelling method can be reliably assessed. Also, the correctness of the material properties should be assured.

Despite the previously mentioned factors, the results are promising and the research should be continued to validate these results. **TJ**

ACKNOWLEDGEMENTS

The main part of this work was carried out in the research project "Termo – Geometry control of the nip rolls in the paper machine environment," financed by the Technology Development Centre of Finland (TEKES) and the Finnish paper industry. The contributions and cooperation of the companies and their staff are gratefully acknowledged.

LITERATURE CITED

1. SHW Casting Technologies, "Steel Rolls?", Technical News Letter, Calender Rolls, No. 13, SHW Casting Technologies GmbH, Aalen-Wasseralfingen, Germany, December 2004
2. Jacot, A., Maijer, D., and Cockcroft, S., *Metall. Mater. Trans. A* 31A(4): 1201(2000).
3. Jacot, A., Maijer, D., and Cockcroft, S., *Metall. Mater. Trans. A* 31A(8): 2059(2000).
4. Widmaier, T., Pirttiniemi, J., Kiviluoma, P., et al., *DAAAM International Scientific Book*, DAAAM International, Vienna, Austria, 2011, pp. 347-364.
5. Rothenbacher, P. and Vomhoff, E., *Tappi J.* 68(7): 82(1985).
6. D'Amato, D., "Temperature controlled rolls design and application," *Prepr. Pap., Annu. Meet. - Can. Pulp Pap. Assoc., Tech. Sect., Part A*, CPPA/PAPTAC, Montreal, 1987.
7. Jokio, M., Ed., *Papermaking Science and Technology, Papermaking Part 3, Finishing,* Fapet Oy, Helsinki, 1999.
8. Wirtz, W., "Advanced thermo rolls for high speed modern calenders," *Int. Conf. New Available Technologies, 7th*, SPCI, Stockholm, 2002.
9. Zaoralek, M., "Hot rolls for soft calendering: Meeting the operator's needs," *TAPPI Finish. Converting Conf.*, TAPPI Press, Atlanta, GA, USA, 1990.
10. Zaoralek, M., "Improved high temperature calender roll," *Prepr. Pap., Annu. Meet. - Can. Pulp Pap. Assoc., Tech. Sect., Part B*, CPPA/PAPTAC, Montreal, 1991.

ABOUT THE AUTHORS

The basis of this paper was a research project in our department at the Aalto University School of Engineering. It complements well our previous research on paper machine rolls, although thermo rolls and their properties were unfamiliar to our research group. We interviewed thermo roll experts and gathered the required information from them and from previous research.

The most interesting aspect of this work was the unique behavior of the thermal effects on the thermo roll. Our most interesting finding was that the bending direction of the roll changes.

Roll suppliers and mills will find this research useful in the manufacturing of better thermo rolls, and we plan to continue studying them.

Widmaier is a post-doctoral research scientist, Kiviluoma is senior university lecturer, and Kuosmanen is professor in the Department of Mechanical Engineering, Aalto University School of Engineering, Aalto, Finland. Pirttiniemi is CEO and Porkka is chief engineer, Dynator Oy, Helsinki, Finland. Email Widmaier at Thomas.Widmaier@aalto.fi.

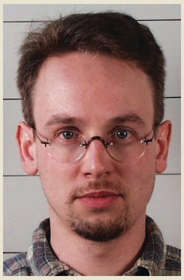

Widmaier

Kiviluoma

Kuosmanen

Pirttiniemi

Porkka

11. Grosskreutz, M., "Thermo rolls – Different flow principles, design according to FKM and alternative materials for best performance in paper calenders," *Asian Paper 2010 – New Appl. Technol. (NAT) Conf.*, UBM, London, 2010.
12. Schweinichen, J., U.S. pat. 6793008 B2 (Sept. 21, 2004).
13. Kiviluoma, P., "Method and device for in situ runout measurement of calender thermo rolls," Ph.D. dissertation, Helsinki University of Technology, Espoo, Finland, 2009.
14. Zaoralek, M., "Higher precision for high temperature calender rolls," *Prepr. Pap., Annu. Meet. - Can. Pulp Pap. Assoc., Tech. Sect., Part B*, CPPA/PAPTAC, Montreal, 2004.
15. Brierley, P., Hopkins, H.G., and Peel, J.D., *Pap. Technol. Ind.* 18(7): 219(1977).
16. Zwart, J. and Farrel, W.R., *Pulp Pap. Can.* 93(2): T41(1992).
17. Neste Oil, "Thermal oil Neste S8," data sheet, Neste Oil, Espoo, Finland.
18. Yovanovich, M.M., "Thermal contact conductance of turned surfaces," *Aerosp. Sci. Meet., 9th*, American Institute of Aeronautics and Astronautics, Reston, VA, USA, 1971.
19. Cooley, J.W. and Tukey, J.W., *Math. Comput.* 19(90): 297(1965).
20. Mosier-Boss, P.A., Liebermann, S.H., and Newbery R., *Appl. Spectrosc.* 49(5): 630(1995).
21. Anderson, J., "Steps in the right direction," Customer Newsletter, SHW Casting Technologies GmbH, Aalen-Wasseralfingen, Germany, 2006, p. 21.
22. Porkka, E., Toiva, J., and Kuosmanen, P., "Run-out of a calender thermo roll at different speeds and temperatures," *Reports in Machine Design 4/2004*, Helsinki University of Technology, Espoo, Finland, 2004.
23. Pirttiniemi, J., Widmaier, T., Kiviluoma, P., et al., "Geometry control of the nip rolls in a paper machine environment - project report," TKK-K-3/09, Publications in Engineering Design and Production, Espoo, Finland, 2009.